

## Corrosion Inhibition of C38 Steel in Acidic Medium Using N-1 Naphthylethylenediamine Dihydrochloride Monomethanolate

H. Zarrok<sup>1</sup>, A. Zarrouk<sup>2,\*</sup>, R. Salghi<sup>4</sup>, M. Ebn Touhami<sup>3</sup>, H. Oudda<sup>1</sup>, B. Hammouti<sup>2</sup>, R. Tourir<sup>3</sup>, F. Bentiss<sup>5</sup>, S. S. Al-Deyab<sup>6</sup>

<sup>1</sup> Laboratoire des procédés de séparation, Faculté des Sciences, Université Ibn Tofail BP 242, 14000 Kénitra, Morocco.

<sup>2</sup> LCAE-URAC18, Faculté des Sciences, Université Mohammed I<sup>er</sup> B.P. 717, 60000 Oujda, Morocco.

<sup>3</sup> Laboratoire d'électrochimie, de corrosion et d'environnement, Faculté des Sciences, Université Ibn Tofail BP 242, 14000 Kenitra, Morocco.

<sup>4</sup> Equipe d'Analyse Agroalimentaire, Ecole Supérieure de Technologie d'Agadir, B.P. 33/S, Agadir, Morocco.

<sup>5</sup> Laboratoire de Chimie de Coordination et d'Analytique (LCCA), Faculté des Sciences, Université Chouaib Doukkali, B.P. 20, M-24000 El Jadida, Morocco.

<sup>6</sup> Petrochemical Research Chair, Chemistry Department, College of Science, King Saud University, P.O. Box 2455, Riyadh 11451, Saudi Arabia.

\*E-mail: [azarrouk@gmail.com](mailto:azarrouk@gmail.com)

Received: 10 January 2013 / Accepted: 25 February 2013 / Published: 1 April 2013

---

The corrosion inhibition effect of N-1-Naphthylethylenediamine Dihydrochloride Monomethanolate (N-NEDHME) as a new inhibitor was studied using electrochemical polarisation, electrochemical impedance spectroscopy (EIS) measurements and weight loss methods. N-NEDHME revealed good corrosion inhibition efficiency even at low concentrations towards C38 steel in HCl medium. Results showed that this compound acts as a mixed type inhibitor. As the inhibitor concentration increased, the charge transfer resistance of C38 steel increased and double layer capacitance decreased. Data, obtained from EIS measurements, were analyzed to model the corrosion inhibition process through appropriate equivalent circuit model, a constant phase element (CPE) has been used. It was found that this inhibitor acts through adsorption on the metal surface. Also, adsorption obeys the Langmuir isotherm with a standard free energy of adsorption ( $\Delta G_{ads}^{\circ}$ ) of  $-40.81 \text{ kJ mol}^{-1}$ . Kinetic parameters (activation energy, pre-exponential factor, enthalpy of activation and entropy of activation) were calculated and discussed. E (%) values obtained from various methods used are in good agreement.

---

**Keywords:** Steel, Hydrochloric acid, Inhibitor, Polarisation curves, EIS, Adsorption.

## 1. INTRODUCTION

C-steel is the most widely used as constructional material in many industries due to its excellent mechanical and low cost. It is used in large tonnages in marine applications, chemical processing, petroleum production and refining, construction and metal processing equipment. Acid solutions are widely used in industry, e.g., chemical cleaning, descaling, pickling, and oil-well acidizing, which leads to corrosive attack. Therefore, the consumption of inhibitors to reduce corrosion has increased in recent years. The corrosion controls by inhibitors is one of the most common effective and economic methods to protect metals in acid media [1-19]. The majority of the well-known inhibitors are organic compounds containing heteroatom, such as O, N, or S and multiple bonds, which allow an adsorption on the metal surface [20-27]. Recently, the excellent inhibitory effect obtained by N-1-Naphthylethylenediamine Dihydrochloride Monomethanolate (N-NEDHME) [28] on copper corrosion in nitric acid, This encouraged us to test this compound in inhibition of corrosion of steel in HCl. In this work, the inhibiting action of N-NEDHME compound (Fig. 1) on the corrosion C38 steel in 1.0 M HCl solution has been investigated. The gravimetric and electrochemical techniques such as potentiodynamic polarization, and impedance measurements were used in this study.

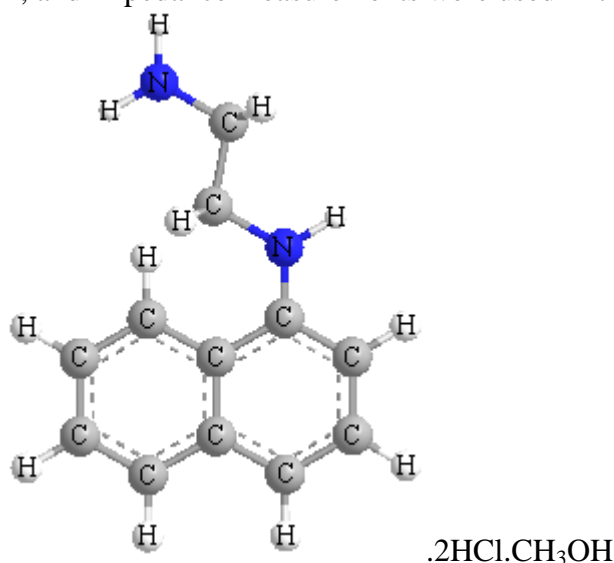


**Figure 1.** The molecular structure of N-NEDHME.

## 2. EXPERIMENTAL METHODS

### 2.1. Materials

The steel used in this study is a carbon steel (Euronorm: C35E carbon steel and US specification: SAE 1035) with a chemical composition (in wt%) of 0.370 % C, 0.230 % Si, 0.680 % Mn, 0.016 % S, 0.077 % Cr, 0.011 % Ti, 0.059 % Ni, 0.009 % Co, 0.160 % Cu and the remainder iron (Fe). The carbon steel samples were pre-treated prior to the experiments by grinding with emery paper SiC (120, 600 and 1200); rinsed with distilled water, degreased in acetone in an ultrasonic bath immersion for 5 min, washed again with bidistilled water and then dried at room temperature before

use. The acid solutions (1.0 M HCl) were prepared by dilution of an analytical reagent grade 37 % HCl with double-distilled water.

### 2.3. Measurements

#### 2.3.1. Weight loss measurements

The steel sheets of  $1.6 \times 1.6 \times 0.07$  cm dimensions were abraded with different grades of emery papers, washed with distilled water, degreased with acetone, dried and kept in a desiccator. After weighing accurately by a digital balance with high sensitivity the specimens were immersed in solution containing 1.0 M HCl solution with and without various concentrations of the investigated inhibitor. At the end of the tests, the specimens were taken out, washed carefully in ethanol under ultrasound until the corrosion products on the surface of carbon steel specimens were removed thoroughly, and then dried, weighed accurately. Duplicate experiments were performed in each case and the mean value of the weight loss is reported. Weight loss allowed calculation of the mean corrosion rate in  $\text{mg cm}^{-2} \text{h}^{-1}$ .

#### 2.3.2. Electrochemical measurements

The electrochemical measurements were carried out using Volta lab (Tacussel- Radiometer PGZ 100) potentiostat and controlled by Tacussel corrosion analysis software model (Voltmaster 4) at under static condition. The corrosion cell used had three electrodes. The reference electrode was a saturated calomel electrode (SCE). A platinum electrode was used as auxiliary electrode of surface area of  $1 \text{ cm}^2$ . The working electrode was carbon steel. All potentials given in this study were referred to this reference electrode. The working electrode was immersed in test solution for 30 minutes to establish steady state open circuit potential ( $E_{\text{ocp}}$ ). After measuring the  $E_{\text{ocp}}$ , the electrochemical measurements were performed. All electrochemical tests have been performed in aerated solutions at 308 K. The polarization curves were obtained in the potential range from -800 to 0 mV(SCE) with  $1 \text{ mV s}^{-1}$  scan rate. The EIS experiments were conducted in the frequency range with high limit of 100 kHz and different low limit 0.1 Hz at open circuit potential, with 10 points per decade, at the rest potential, after 30 min of acid immersion, by applying 10 mV ac voltage peak-to-peak. Nyquist plots were made from these experiments. The best semicircle can be fit through the data points in the Nyquist plot using a non-linear least square fit so as to give the intersections with the  $x$ -axis.

## 3. RESULTS AND DISCUSSION

### 3.1. Polarization curves

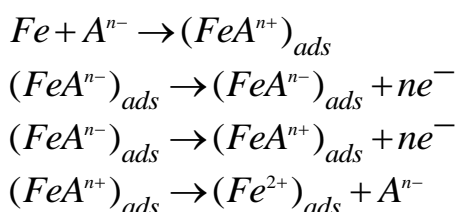
The typical Tafel polarization curves of C38 steel in 1.0 M HCl in the presence and absence of N-NEDHME at different concentrations are shown in Fig. 2. It could be observed that both the

cathodic and anodic reactions were suppressed with the addition of N-NEDHME, which suggests that the N-NEDHME reduced anodic dissolution and also retarded the hydrogen evolution reaction effectively.

Various corrosion kinetics parameters, i.e. corrosion potential ( $E_{\text{corr}}$ ), cathodic Tafel slope ( $\beta_c$ ) and corrosion current density ( $I_{\text{corr}}$ ) obtained from the Tafel extrapolation of the polarization curves, are given in Table 1. The ( $\eta_{\text{Tafel}}$  (%)) is calculated using the following equation [29]:

$$\eta_{\text{Tafel}}(\%) = \left( \frac{I_{\text{corr}} - I'_{\text{corr}}}{I_{\text{corr}}} \right) \times 100 \quad (1)$$

where  $I_{\text{corr}}$  and  $I'_{\text{corr}}$  are uninhibited and inhibited corrosion current densities, respectively. They are determined by extrapolation of Tafel lines to the respective corrosion potentials. Some of the authors proposed the following mechanism for the corrosion of iron and steel in acid solution [30-32]:



The cathodic hydrogen evolution

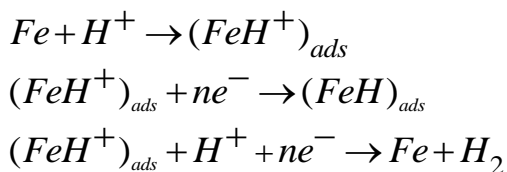


**Table 1.** Electrochemical parameters of C38 steel at various concentrations of N-NEDHME studied in 1.0 M HCl at 308 K.

Inhibitor	Conc (M)	$-E_{\text{corr}}$ (mV/SCE)	$-\beta_c$ (mV/dec)	$I_{\text{corr}}$ ( $\mu\text{A}/\text{cm}^2$ )	$\eta_{\text{Tafel}}$ (%)
Blank	1.0	475.9	175.6	1077.8	-
N-NEDHME	$10^{-3}$	492.9	145.1	88.2	91.8
	$10^{-4}$	472.9	147.7	149.6	86.1
	$10^{-5}$	502.9	182.1	189.9	82.4
	$10^{-6}$	533.5	143.9	247.9	77.0

The obtained results show that the inhibition efficiency increased, while the corrosion current density decreased when the concentration of the inhibitor is increased. This could be explained on the basis of adsorption of N-NEDHME on the C38 steel surface and the adsorption process enhanced with

increasing inhibitor concentration. The data in Table 1 show that increasing N-NEDHME concentration slightly shifts the values of corrosion potential ( $E_{\text{corr}}$ ) in cathodic direction indicating that it acts as mixed-type inhibitor. The cathodic Tafel slope ( $\beta_c$ ) show slight changes with the addition of N-NEDHME, which suggests that the inhibiting action occurred by simple blocking of the available cathodic sites on the metal surface, which lead to a decrease in the exposed area necessary for hydrogen evolution and lowered the dissolution rate with increasing N-1-Naphthylethylenediamine Dihydrochloride Monomethanolate concentration. The parallel cathodic Tafel plots obtained in Fig. 2 indicate that the hydrogen evolution is activation-controlled and the reduction mechanism is not affected by the presence of inhibitor [33].

The inhibitor efficiency values,  $\eta_{\text{Tafel}}(\%)$ , calculated from the  $I_{\text{corr}}$  are presented in Table 1. Inspection of these data shows that the addition of N-NEDHME inhibits the steel corrosion in 1.0 M HCl and the protection efficiency increases with  $C_{\text{inh}}$  reaching its maximum value, 91.8 %, at  $10^{-3}$  M.

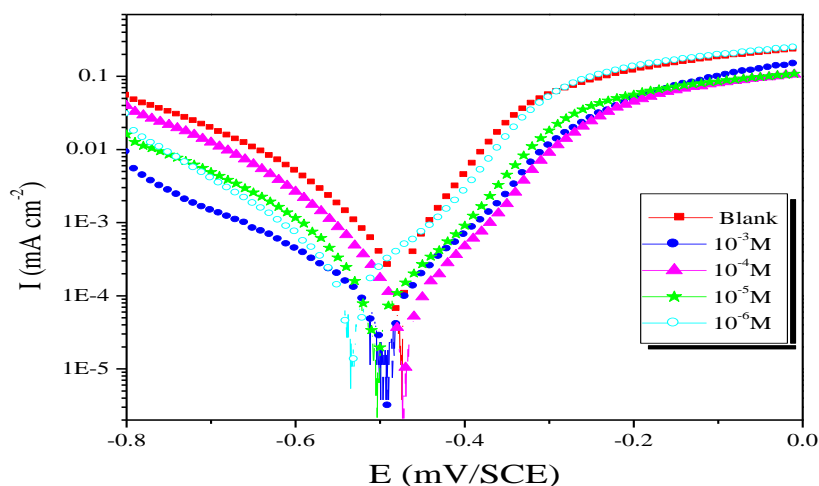


**Figure 2.** Polarization curves for Steel in 1.0 M HCl in the absence and presence of different concentrations of N-NEDHME at 308K.

### 3.2. Electrochemical impedance spectroscopy

The corrosion behaviour of C38-steel in acidic solution in the presence of N-NEDHME was investigated by electrochemical impedance spectroscopy (EIS) at 308 K after 30 min of immersion at corrosion potential. Nyquist plots of steel in inhibited and uninhibited acidic solutions containing various concentrations of N-NEDHME are shown in Fig. 3. The Nyquist plots for all N-NEDHME concentrations are characterized by one semicircular capacitive loop. The presence of inhibitor introduces the diffusion step in corrosion process and the reaction becomes diffusion-controlled. Hence, the corrosion process can have two steps as in any electrochemical process at the electrochemical interface, first, the oxidation of the metal (charge transfer process) and second, the diffusion of the metallic ions from the metal surface to the solution (mass transport process). Inhibitor

gets adsorbed on the electrode surface and thereby produces a barrier for the metal to diffuse out to the bulk and this barrier increases with increasing the inhibitor concentration [34].

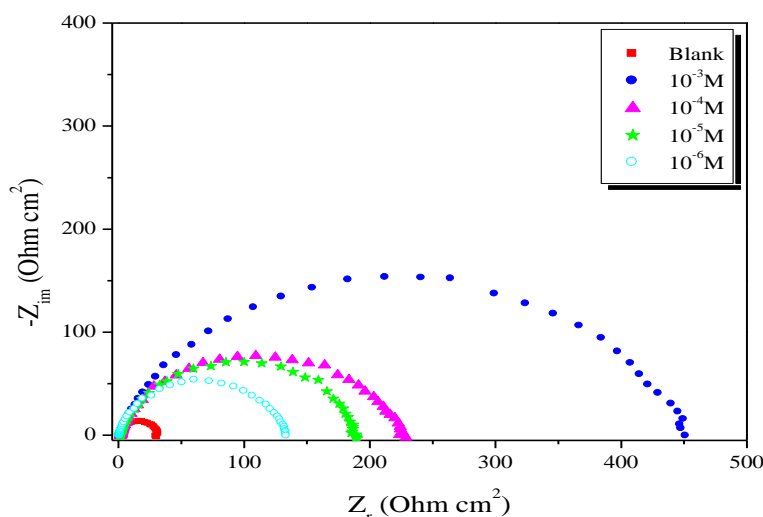


**Figure 3.** Typical Nyquist plots obtained for the C38 steel in 1.0 M HCl in the absence and presence of four different concentrations of N-NEDHME.

The EIS results are simulated by the equivalent circuit shown in Fig. 4 to pure electric models that could verify or rule out mechanistic models and enable the calculation of numerical values corresponding to the physical and/or chemical properties of the electrochemical system under investigation [35]. The circuit employed allows the identification of both solution resistance ( $R_s$ ) and charge transfer resistance ( $R_{ct}$ ). It is worth mentioning that the double layer capacitance ( $C_{dl}$ ) value is affected by imperfections of the surface, and that this effect is simulated via a constant phase element (CPE) [36]. A constant phase element (CPE) is substituted for the capacitive element to give a more accurate fit [37], as the Nyquist plot obtained for this inhibitor present a depressed loop, such behavior is characteristic for solid electrodes and often referred to as frequency dispersion which has been attributed to the surface heterogeneity [38-42]. The CPE impedance is given by [43,44]:

$$Z_{CPE} = A^{-1} (i \omega)^{-n} \tag{2}$$

where A is the CPE constant,  $\omega$  is the angular frequency (in  $\text{rad s}^{-1}$ ),  $i^2 = -1$  is the imaginary number and n is a CPE exponent which can be used as a gauge of the heterogeneity or roughness of the surface [44]. Depending on the value of n, CPE can represent resistance ( $n=0$ ,  $A = R$ ), capacitance ( $n=1$ ,  $A = C$ ), inductance ( $n = -1$ ,  $A = L$ ) or Warburg impedance ( $n = 0.5$ ,  $A = W$ ). The transfer function is thus represented by an equivalent circuit, which has been previously used [44, 45], having only one time constant (Fig. 5). Parallel to the double-layer capacitance (simulated by a CPE) is the charge transfer resistance ( $R_{ct}$ ), and  $R_s$  is the electrolyte resistance. Excellent fit with this model was obtained for all experimental data. As an example, the Nyquist and Bode plots of both experimental and simulated data of carbon steel in 1.0 M HCl solution

containing  $10^{-3}$  M of N-NEDHME are shown in Fig. 4. It is clear that the measured impedance plot is in accordance with that calculated by the used equivalent circuit model. The electrochemical parameters, including  $R_s$ ,  $R_{ct}$ , A and n, obtained from fitting the recorded EIS data using the equivalent circuit of Fig. 5, are listed in Table 3.

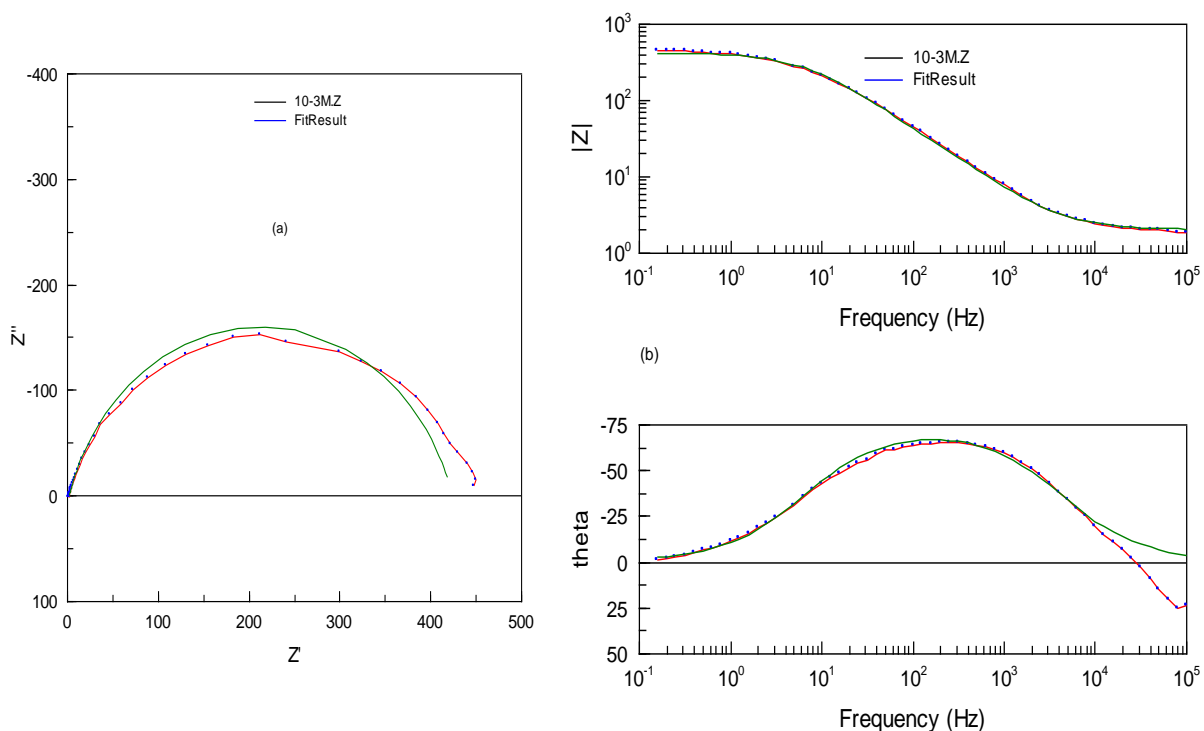


**Figure 4.** EIS Nyquist (a) and Bode (b) plots for carbon steel/1.0 M HCl +  $10^{-3}$  M N-NEDHME interface: (...) experimental data; (—) calculated.

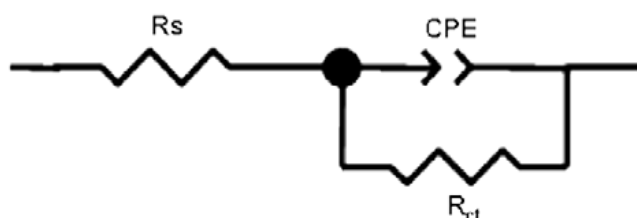


**Figure 5.** Electrical equivalent circuit used to fit the EIS data of the interface carbon steel/1.0 M HCl solution without and with N-NEDHME inhibitor.

In this table are shown also the calculated “double layer capacitance” values,  $C_{dl}$ , derived from the CPE parameters according to [46]:

$$C_{dl} = (AR_{ct}^{1-n})^{1/n} \tag{3}$$

and the relaxation time constants according to the dielectric theory:

$$\tau = \frac{1}{2\pi f_{\max}} \tag{4}$$

where  $f_{\max}$  is the frequency at which appears the maximum in the curve  $-\Phi$  (phase shift) vs.  $\log f$ . The relaxation time of a surface state is the time required for return of the charge distribution to equilibrium after an electrical disturbance, and in the case, when no distributed element is inserted to replace the double layer capacitance, it is defined [47] as:

$$\tau = C_{dl} R_{ct} \tag{5}$$

The inhibition efficiency IE (%) is calculated by  $R_{ct}$  using Eq. (6), where  $R_{ct}^0$  and  $R_{ct}$  are the charge-transfer resistance values without and with inhibitor, respectively:

$$IE(\%) = \frac{1/R_{ct}^0 - 1/R_{ct}}{1/R_{ct}^0} \times 100 \tag{6}$$

**Table 2.** Impedance parameters and inhibition efficiency values for carbon steel in 1.0 M HCl without and with different concentrations of N-NEDHME at 308 K.

Conc (mol L <sup>-1</sup> )	R <sub>s</sub> (Ω cm <sup>2</sup> )	R <sub>ct</sub> (Ω cm <sup>2</sup> )	n	A × 10 <sup>-3</sup> (s <sup>n</sup> Ω <sup>-1</sup> cm <sup>-2</sup> )	C <sub>dl</sub> (μF cm <sup>-2</sup> )	τ (s)	IE (%)
Blank	1.67	29.66	0.91	0.14612	85.31	0.02530	-----
10 <sup>-3</sup>	2.02	421.90	0.83	0.10911	58.08	0.02450	93.0
10 <sup>-4</sup>	1.87	209.0	0.85	0.13350	70.98	0.01485	85.8
10 <sup>-5</sup>	2.02	165.9	0.86	0.14058	76.24	0.01265	82.1
10 <sup>-6</sup>	1.51	121.7	0.88	0.14278	82.16	0.00999	75.6

It is found (Table 2) that, as the N-NEDHME concentration increases, the  $R_{ct}$  values increase, but the  $C_{dl}$  values tend to decrease. The decrease in  $C_{dl}$  values is interpreted by the adsorption of N-NEDHME on the metal surface [48]. It is apparent from Nyquist diagrams that the charge-transfer resistance value of C38 steel in uninhibited 1.0 M HCl solution changes significantly after the addition of the inhibitor. Furthermore,  $C_{dl}$  decreases with increase of the concentration of inhibitor (Fig. 6). This phenomenon is generally related to the adsorption of organic molecules on the metal surface and then leads to a decrease in the local dielectric constant and/or an increase in the thickness of the electrical double layer [49].

$$C_{dl} = \frac{\epsilon_o \epsilon}{\delta} S \tag{7}$$

where  $\delta$  is the thickness of the protective layer,  $S$  is the electrode area,  $\epsilon_0$  the vacuum permittivity of vide and  $\epsilon$  is dielectric constant of the medium.

A low capacitance may result if water molecules at the electrode interface are largely replaced by organic inhibitor molecules through adsorption [50]. The larger inhibitor molecules also reduce the capacitance through the increase in the double layer thickness [51]. The inhibiting effectiveness increases with the concentration of the inhibitor to reach a maximum value from 93.0% to  $10^{-3}$  M.

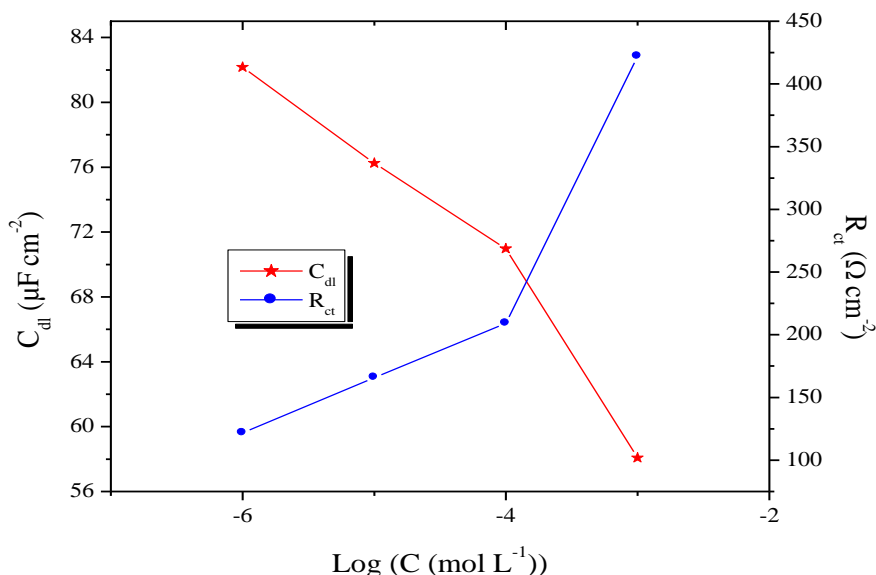


**Figure 6.** Evolution of transfer resistance and capacitance as function of logarithm of N-NEDHME concentration.

### 3.3. Gravimetric study

#### 3.3.1. Effect of N-NEDHME concentration

The effect of addition of N-NEDHME tested at different concentrations on the corrosion of carbon steel in 1.0 M HCl solution was studied by weight loss method at 308 K after 6 h of immersion period. The corrosion rate ( $C_R$ ) and inhibition efficiency  $\eta_{WL}(\%)$  were calculated according to the Eqs. 8 and 9 [52,53], respectively:

$$C_R = \frac{W_b - W_a}{At} \tag{8}$$

$$\eta_{WL}(\%) = \left(1 - \frac{w_i}{w_0}\right) \times 100 \tag{9}$$

where  $W_b$  and  $W_a$  are the specimen weight before and after immersion in the tested solution,  $w_0$  and  $w_i$  are the values of corrosion weight losses of carbon steel in uninhibited and inhibited solutions, respectively,  $A$  the total area of the carbon steel specimen ( $\text{cm}^2$ ) and  $t$  is the exposure time (h).

It is obvious from the Table 3 that the N-NEDHME inhibit the corrosion of C38 steel in 1.0 M HCl solution at all concentrations used in this study and the corrosion rate (w) is seen to decrease continuously with increasing additive concentration at 308K. Indeed, corrosion rate values of C38 steel decrease when the inhibitor concentration increases while  $\eta_{WL}(\%)$  values of N-NEDHME increase with the increase of the concentration, the maximum  $\eta_{WL}(\%)$  of 96% is achieved at  $10^{-3}$  M of N-NEDHME. The high inhibitive performance of N-NEDHME suggests a higher bonding of this compound to the surface, which posses higher number of lone pairs from heteroatom and  $\pi$ -orbitals.

**Table 3.** Weight loss results for C38 steel in 1.0 M HCl in the absence and presence of N-NEDHME at various concentrations.

Inhibitor	Con (M)	$C_R(\text{mg cm}^{-2} \text{h}^{-1})$	$\eta_{WL}(\%)$	$\theta$
Blank	1	1.07	-	
	$1 \times 10^{-3}$	0.045	95.8	0.958
	$5 \times 10^{-4}$	0.090	91.6	0.916
	$1 \times 10^{-4}$	0.127	88.1	0.881
N-NEDHME	$5 \times 10^{-5}$	0.171	84.0	0.840
	$1 \times 10^{-5}$	0.201	81.2	0.812
	$1 \times 10^{-6}$	0.308	71.2	0.712

The evolution of both the corrosion rates and the inhibition efficiencies evaluated from weight loss measurements for different N-NEDHME concentrations in 1.0 M HCl is illustrated in Fig 7. The addition of N-NEDHME diminished the corrosion rate and hence inhibited C38 steel corrosion in acid solution. The decrease in CR with increasing inhibitor concentration suggests that the inhibiting action was concentration dependent. The inhibition efficiency ( $\eta_{WL}(\%)$ ) attained its maximum (95.8%) at  $10^{-3}$ M.

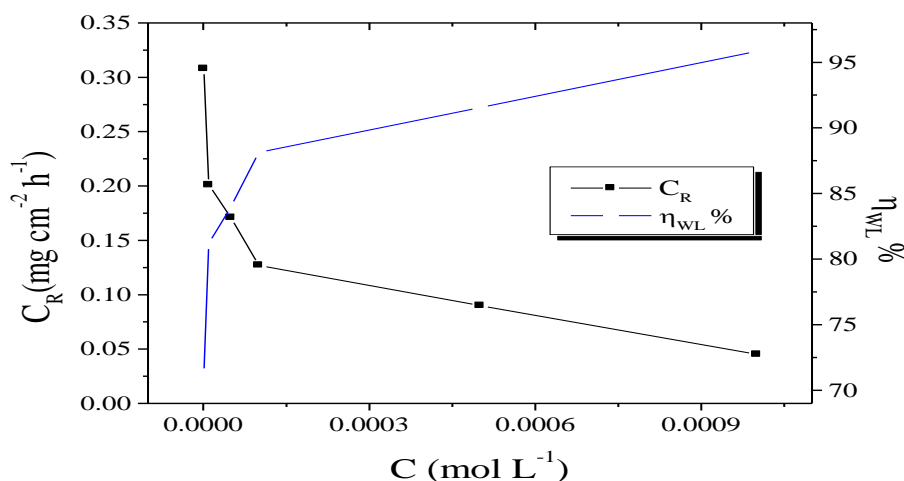


**Figure 7.** Variation of the corrosion rate and inhibitive efficiency against the N-NEDHME concentrations.

The results show that the inhibition efficiencies increase with increasing inhibitor concentration. The results obtained from the weight loss measurements are in good trend agreement with those obtained from the electrochemical methods.

### 3.3.2. Effect of temperature

The effect of temperature on the corrosion parameters of carbon steel in free and inhibited solutions of 1.0 M HCl was studied at a temperature range of 308-343K. Acid solutions were inhibited by adding different concentrations of inhibitor. The obtained corrosion parameters are given in Table 4 and show when temperature increases, in the absence and presence of inhibitor, the corrosion rate increases. Data in Table 4 revealed that the investigated N-NEDHME exhibited inhibition properties at all the studied temperatures and the values of  $\eta_{WL}(\%)$  decreases with increasing temperature.

**Table 4.** Various corrosion parameters for C38 steel in 1.0 M HCl in absence and presence of optimum concentration of N-NEDHME at different temperatures.

Temp (K)	Inhibitor	$C_R$ ( $\text{mg cm}^{-2} \text{h}^{-1}$ )	$\eta_{WL}$ (%)	$\theta$
	Blank	1.070	-	-
308	N-NEDHME	0.045	95.8	0.958
	Blank	1.490	-	-
313	N-NEDHME	0.092	93.8	0.938
	Blank	2.870	-	-
323	N-NEDHME	0.281	90.2	0.902
	Blank	5.210	-	-
333	N-NEDHME	0.740	85.8	0.858
	Blank	10.02	-	-
343	N-NEDHME	2.044	79.6	0.796

In order to calculate the activation energy of the corrosion process and investigation of the mechanism of inhibition, gravimetric measurements were carried out at various temperatures (308–343K) in the absence and presence of N-NEDHME in 1.0 M HCl. The dependence of the corrosion rate on temperature can be expressed by the Arrhenius equation. The Arrhenius equation could be written by Eq. (10) [54]:

$$C_R = A \exp\left(\frac{-E_a}{RT}\right) \quad (10)$$

where  $C_R$  is the corrosion rate, R the gas constant, T the absolute temperature, A the pre-exponential factor. Using the logarithm:

$$\ln C_R = \frac{-E_a}{RT} + \ln A \quad (11)$$

The Arrhenius plot and transition state plot were used to determine the activation energy ( $E_a$ ), activation enthalpy ( $\Delta H_a$ ), and activation entropy ( $\Delta S_a$ ) for the corrosion of C38 steel in 1.0 M HCl with and without N-NEDHME. The activation energy can be obtained by the Arrhenius equation and Arrhenius plot:

The graph of  $\ln(C_R)$  against  $1/T$  gives a straight line with a slope of  $(-E_a/R)$ . Fig. 8 shows the Arrhenius plot for C38 steel in 1M HCl with the presence and absence of N-NEDHME.  $E_a$  was calculated and tabulated in Table 5. The transition state equation was used to calculate the  $\Delta H_a$  and  $\Delta S_a$  :

$$C_R = \frac{RT}{Nh} \exp\left(\frac{\Delta S_a}{R}\right) \exp\left(-\frac{\Delta H_a}{RT}\right) \quad (12)$$

where  $N$  is Avogadro's number ( $6.02 \times 10^{23} \text{ mol}^{-1}$ ) and  $h$  is Plank's constant ( $6.63 \times 10^{-34} \text{ m}^2 \text{ kg s}^{-1}$ ). Eq. (12) looks like an exponential multiplied by a factor that is linear in temperature.

However, the activation energy is itself a temperature dependent quantity as follows:

$$E_a = \Delta H_a - T\Delta S_a \quad (13)$$

Therefore, when all of the details are worked out one ends up with an expression that again takes the form of an Arrhenius exponential multiplied by a slowly varying function of  $T$ . The precise form of the temperature dependence depends upon the reaction, and can be calculated using formulas from statistical mechanics involving the partition functions of the reactants and of the activated complex. Nevertheless, in order to carry simple calculations, Eq. (13) was rearranged to become:

$$\ln(C_R/T) = \left(\frac{-\Delta H_a}{RT}\right) + \left[\ln\left(\frac{R}{Nh}\right) + \frac{\Delta S_a}{R}\right] \quad (14)$$

A plot of  $\ln(C_R/T)$  against  $1/T$  should give a straight line with a slope of  $(-\Delta H_a/R)$  and intercept of  $[\ln(R/Nh) + (\Delta S_a/R)]$ , as shown in Fig. 9.  $\Delta H_a$  and  $\Delta S_a$  were calculated and tabulated in Table 5. From Table 5, the activation energy  $E_a$  increases in the presence of the inhibitor. Increases in  $E_a$  with the presence of N-NEDHME indicate that a physical (electrostatic) adsorption occurred in the first stage. N-NEDHME is an organic nitrogen compound that easily protonates to give a cationic form in acid medium. The  $E_a$  value was greater than  $20 \text{ kJ mol}^{-1}$  in both the presence and absence of the inhibitor, which reveals that the entire process is controlled by the surface reaction [55].

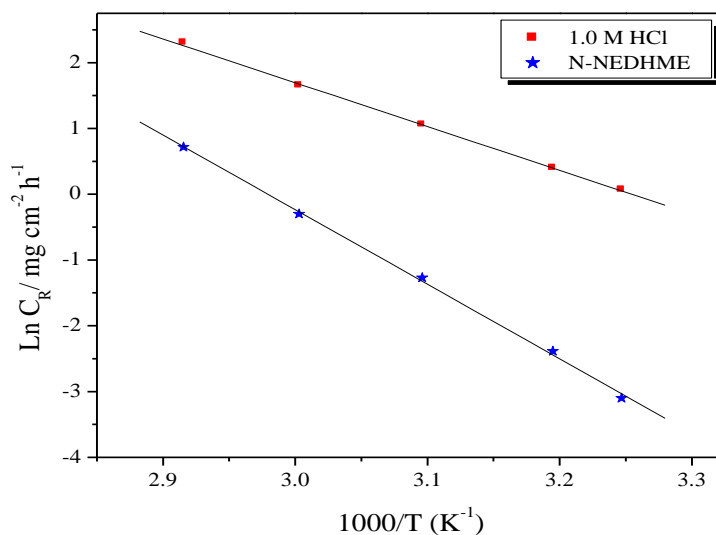


**Figure 8.** Arrhenius plots of  $\text{Ln } C_R$  vs.  $1/T$  for steel in 1.0 M HCl in the absence and the presence of N-NEDHME at optimum concentration.

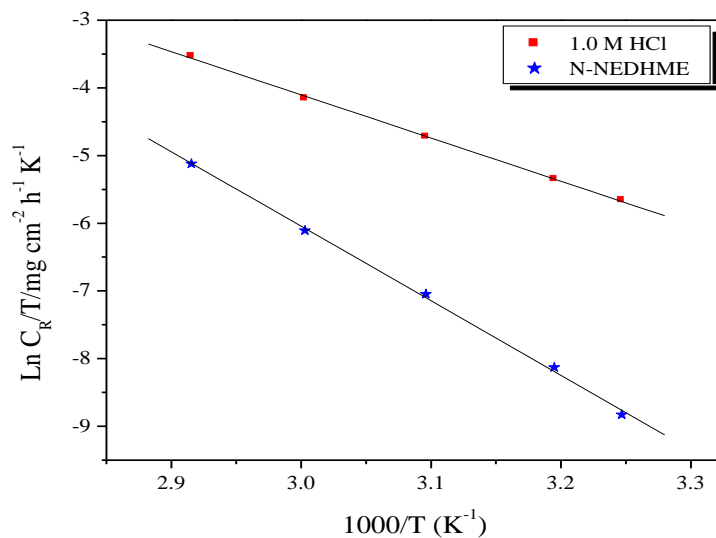


**Figure 9.** Arrhenius plots of  $\text{Ln } C_R/T$  vs.  $1/T$  for steel in 1.0 M HCl in the absence and the presence of N-NEDHME at optimum concentration.

**Table 5.** The values of activation parameters for C38 steel in 1.0 M HCl in the absence and the presence of different concentrations of N-NEDHME.

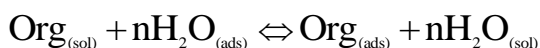
Inhibitor	A (mg/cm <sup>2</sup> h)	Linear regression coefficient (r)	$E_a$ (kJ/mol)	$\Delta H_a$ (kJ/mol)	$\Delta S_a$ (J/mol K)
Blank	$3.0066 \times 10^9$	0.99961	55.75	53.05	-72.49
N-NEDHME	$4.6698 \times 10^{14}$	0.99936	94.26	91.56	26.88

The values of  $\Delta H_a$  and  $E_a$  are nearly the same and are higher in the presence of the inhibitor. This indicates that the energy barrier of the corrosion reaction increased in the presence of the inhibitor without changing the mechanism of dissolution. The positive values of  $\Delta H_a$  for both corrosion processes with and without the inhibitor reveal the endothermic nature of the steel dissolution process and indicate that the dissolution of steel is difficult [27, 56].

The large negative value of  $\Delta S_a$  for C38 steel in 1.0 M HCl implies that the activated complex is the rate-determining step, rather than the dissociation step. In the presence of the inhibitor, the value of  $\Delta S_a$  increases and is generally interpreted as an increase in disorder as the reactants are converted to the activated complexes [27]. The positive values of  $\Delta S_a$  reflect the fact that the adsorption process is accompanied by an increase in entropy, which is the driving force for the adsorption of the inhibitor onto the steel surface.

### 3.3.3. Adsorption isotherm and thermodynamic parameters

It is well established that the first step in corrosion inhibition of metals and alloys is the adsorption of organic inhibitor molecules at the metal/solution interface and that the adsorption depends on the molecule's chemical composition, the temperature and the electrochemical potential at the metal/solution interface. In fact, the solvent water molecules could also adsorb at metal/solution interface. So the adsorption of organic inhibitor molecules from the aqueous solution can be regarded as a quasi-substitution process between the organic compounds in the aqueous phase [Org(sol)] and water molecules at the electrode surface [H<sub>2</sub>O(ads)] [57].



where Org(sol) and Org(ads) are the organic specie dissolved in the aqueous solution and adsorbed onto the metallic surface, respectively, H<sub>2</sub>O(ads) is the water molecule adsorbed on the metallic surface and n is the size ratio representing the number of water molecules replaced by one organic adsorbate.

Basic information on the interaction between the inhibitor and the alloy surface can be provided by the adsorption isotherm. In order to obtain the isotherm, the fractional coverage values  $\theta$  as a function of inhibitor concentration ( $C_{\text{inh}}$ ) must be obtained. It is well known that  $\theta$  can be obtained from the  $\theta = \eta_{\text{WL}}(\%)/100$  ratio. Attempts were made to fit the  $\theta$  values to various isotherms including Langmuir, Temkin, Frumkin and Flory-Huggins. Many adsorption isotherms were plotted and the Langmuir adsorption isotherm was found to be the best description of the adsorption behavior of the studied inhibitors. According to this isotherm,  $\theta$  is related to equilibrium adsorption constant ( $K_{\text{ads}}$ ) and  $C_{\text{inh}}$  by the relation

$$\frac{C_{\text{inh}}}{\theta} = \frac{1}{K_{\text{ads}}} + C_{\text{inh}} \quad (9)$$

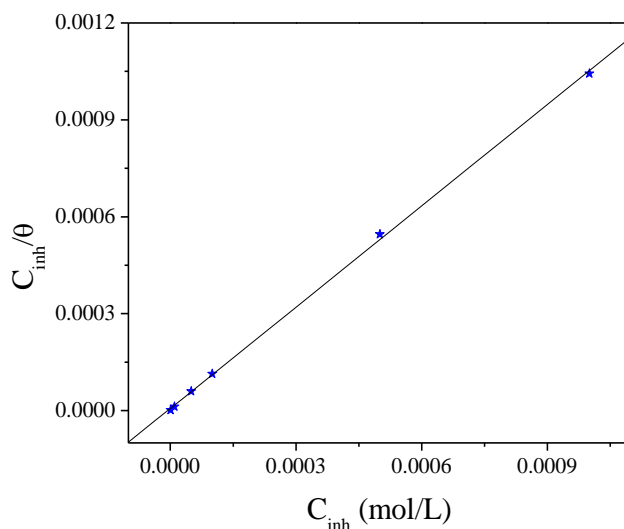


**Figure 8.** Langmuir isotherm adsorption model of N-NEDHME on the surface of C38 steel in 1.0 M HCl.

Figure 8 shows the plot of  $C_{inh}/\theta$  vs.  $C_{inh}$  and the expected linear relationship is obtained. The value of regression coefficient ( $R^2$ ) confirmed the validity of this approach. The slope of this straight line is 0.99976, suggesting that adsorbed inhibitor molecules form monolayer on the C38 steel surface and there is no interaction among the adsorbed inhibitor molecules. On the other hand, the equilibrium constant of adsorption is related to the standard energy of adsorption ( $\Delta G_{ads}^\circ$ ) by the relation [58]

$$K_{ads} = \left(\frac{1}{55.5}\right) \exp\left(-\frac{\Delta G_{ads}^\circ}{RT}\right) \tag{10}$$

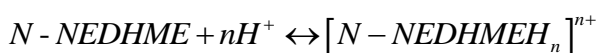
where R is the universal gas constant, T the absolute temperature and the value of 55.5 is the concentration of water in  $\text{mol.L}^{-1}$  in the solution [59].

The thermodynamic parameters for adsorption process obtained from Langmuir adsorption isotherm for the studied N-1-Naphthylethylenediamine Dihydrochloride Monomethanolate molecule is given in Table 4. The negative value of  $\Delta G_{ads}^\circ$  and the higher value of  $K_{ads}$  reveal the spontaneity of adsorption process and they are characteristic of strong interaction and stability of the adsorbed layer with the steel surface.

**Table 4.** Thermodynamic parameters for the adsorption of N-NEDHME in 1.0 M HCl on the C38 steel at 308K.

Inhibitor	Slope	$K_{ads}$ ( $M^{-1}$ )	$R^2$	$\Delta G_{ads}^\circ$ (KJ/mol)
N-NEDHME	1.04	150601.73	0.99976	-40.81

Generally, the standard free energy values of  $-20 \text{ kJ mol}^{-1}$  or less negative are associated with an electrostatic interaction between charged molecules and charged metal surface (physical adsorption); those of  $-40 \text{ kJ mol}^{-1}$  or more negative involves charge sharing or transfer from the inhibitor molecules to the metal surface to form a co-ordinate covalent bond (chemical adsorption) [60, 61]. The calculated standard free energy of adsorption value is closer to  $-40 \text{ kJ mol}^{-1}$ . This value is in frontier between the two mode of adsorption, therefore, it can be concluded that the adsorption is a competitive phenomenon between chemical and physical adsorption [32,62]. However, N-NEDHME contains two nitrogen atoms which are easily protonated in HCl solution. Therefore, physical adsorption is possible via electrostatic interaction between a negatively charged surface, which is provided with a specifically adsorbed chloride anion on steel, and the positive charge of the inhibitor [63]. Generally, Corrosion inhibition mechanism in acid medium is the adsorption of inhibitor onto the metal surface. As far as the inhibition process is concerned, it is generally assumed that adsorption of the inhibitor at the metal/solution interface is the first step in the action mechanism of the inhibitors in aggressive acid media. Four types of adsorption may take place during inhibition involving organic molecules at the metal/solution inter-face: (1) electrostatic attraction between charged molecules and the charged metal, (2) interaction of unshared electron pairs in the molecule with the metal, (3) interaction of  $\pi$ -electrons with the metal, and (4) a combination of the above [64]. Concerning inhibitors, the inhibition efficiency depends on several factors; such as the number of adsorption sites and their charge density, molecular size, heat of hydrogenation, mode of interaction with the metal surface, and the formation metallic complexes [65]. Physical adsorption requires presence of both electrically charged surface of the metal and charged species in the bulk of the solution; the presence of a metal having vacant low-energy electron orbital and of an inhibitor with molecules having relatively loosely bound electrons or heteroatom with lone pair electrons. However, the compound reported can be protonated in an acid medium. Thus they become cations, existing in equilibrium with the corresponding molecular form:



The protonated N-NEDHME, however, could be attached to the C38steel surface by means of electrostatic interaction between  $\text{Cl}^-$  and protonated N-NEDHME since the C38 steel surface has positive charge in the HCl medium [66]. This could further be explained based on the assumption that in the presence of  $\text{Cl}^-$ , the negatively charged  $\text{Cl}^-$  would attach to positively charged surface

#### 4. CONCLUSIONS

N-1-Naphthylethylenediamine Dihydrochloride Monomethanolate (N-NEDHME) was an effective inhibitor for corrosion of C38 steel in 1.0 M hydrochloric acid, and the inhibition efficiency increased with increasing in the inhibitor concentration. N-NEDHME gave >71% protection to C38 steel in 1.0 M HCl at a concentration as low as  $10^{-6}\text{M}$ . In addition, its protection was > 95% at  $10^{-3}\text{M}$  concentration of inhibitor. N-NEDHME acted as a mixed type inhibitor. EIS results showed that as the

inhibitor concentration increased the charge transfer resistance increased and the double layer capacity decreased. The inhibition efficiencies increased with increasing inhibitor concentration but decreased with temperature. N-NEDHME acted through adsorption on the C38 steel surface and its adsorption obeyed the Langmuir adsorption isotherm. The values of free Gibbs energy showed that Compound was adsorbed on the steel surface via chemical and physical adsorption. Inhibition efficiencies obtained from weight loss experiments were in good trend agreement with other methods.

#### ACKNOWLEDGEMENTS

Prof S. S. Al-Deyab and Prof B. Hammouti extend their appreciation to the Deanship of Scientific Research at King Saud University for funding the work through the research group project.

#### References

1. A. K. Singh, M. A. Quraishi, *J. Mater. Environ. Sci.* 1 (2) (2010) 101.
2. D.D.N. Singh, T.B. Singh, B. Gaur, *Corros. Sci.* 37 (1995) 1005.
3. M. Prajila, J. Sam, J. Bincy, J. Abraham, *J. Mater. Environ. Sci.* 3 (6) (2012) 1045.
4. U.J. Naik, V.A. Panchal, A.S. Patel, N.K. Shah, *J. Mater. Environ. Sci.* 3 (5) (2012) 935.
5. A. Zarrouk, H. Zarrok, R. Salghi, B. Hammouti, F. Bentiss, R. Touir, M. Bouachrine, *J. Mater. Environ. Sci.* 4 (2) (2013) 177.
6. H. Zarrok, H. Oudda, A. Zarrouk, R. Salghi, B. Hammouti, M. Bouachrine, *Der Pharm. Chem.* 3 (2011) 576.
7. H. Zarrok, R. Salghi, A. Zarrouk, B. Hammouti, H. Oudda, Lh. Bazzi, L. Bammou, S. S. Al-Deyab, *Der Pharm. Chem.* 4 (2012) 407.
8. H. Zarrok, S. S. Al-Deyab, A. Zarrouk, R. Salghi, B. Hammouti, H. Oudda, M. Bouachrine, F. Bentiss, *Int. J. Electrochem. Sci.* 7 (2012) 4047.
9. D. Ben Hmamou, R. Salghi, A. Zarrouk, H. Zarrok, B. Hammouti, S. S. Al-Deyab, M. Bouachrine, A. Chakir, M. Zougagh, *Int. J. Electrochem. Sci.* 7 (2012) 5716.
10. A. Zarrouk, B. Hammouti, S.S. Al-Deyab, R. Salghi, H. Zarrok, C. Jama, F. Bentiss, *Int. J. Electrochem. Sci.* 7 (2012) 5997.
11. A. Zarrouk, H. Zarrok, R. Salghi, B. Hammouti, S.S. Al-Deyab, R. Touzani, M. Bouachrine, I. Warad, T. B. Hadda, *Int. J. Electrochem. Sci.* 7 (2012) 6353.
12. A. Zarrouk, M. Messali, H. Zarrok, R. Salghi, A. Al-Sheikh Ali, B. Hammouti, S. S. Al-Deyab, F. Bentiss, *Int. J. Electrochem. Sci.* 7 (2012) 6998.
13. H. Zarrok, A. Zarrouk, R. Salghi, Y. Ramli, B. Hammouti, S. S. Al-Deyab, E. M. Essassi, H. Oudda, *Int. J. Electrochem. Sci.* 7 (2012) 8958.
14. D. Ben Hmamou, R. Salghi, A. Zarrouk, H. Zarrok, S. S. Al-Deyab, O. Benali, B. Hammouti, *Int. J. Electrochem. Sci.* 7 (2012) 8988.
15. A. Zarrouk, M. Messali, M. R. Aouad, M. Assouag, H. Zarrok, R. Salghi, B. Hammouti, A. Chetouani, *J. Chem. Pharm. Res.* 4 (2012) 3427.
16. D. Ben Hmamou, M. R. Aouad, R. Salghi, A. Zarrouk, M. Assouag, O. Benali, M. Messali, H. Zarrok, B. Hammouti, *J. Chem. Pharm. Res.* 4 (2012) 3489.
17. H. Zarrok, H. Oudda, A. El Midaoui, A. Zarrouk, B. Hammouti, M. Ebn Touhami, A. Attayibat, S. Radi, R. Touzani, *Res. Chem. Intermed* (2012) DOI 10.1007/s11164-012-0525-x
18. A. Zarrouk, B. Hammouti, H. Zarrok, R. Salghi, A. Dafali, Lh. Bazzi, L. Bammou, S. S. Al-Deyab, *Der Pharm. Chem.* 4 (2012) 337
19. A. Zarrouk, A. Dafali, B. Hammouti, H. Zarrok, S. Boukhris, M. Zertoubi, *Int. J. Electrochem. Sci.* 5 (2010) 46.

20. A. Zarrouk, T. Chelfi, A. Dafali, B. Hammouti, S.S. Al-Deyab, I. Warad, N. Benchat, M. Zertoubi, *Int. J. Electrochem. Sci.* 5 (2010) 696.
21. A. Zarrouk, I. Warad, B. Hammouti, A. Dafali, S.S. Al-Deyab, N. Benchat, *Int. J. Electrochem. Sci.* 5 (2010) 1516.
22. A. Zarrouk, B. Hammouti, R. Touzani, S.S. Al-Deyab, M. Zertoubi, A. Dafali, S. Elkadiri, *Int. J. Electrochem. Sci.* 6 (2011) 4939.
23. A. Zarrouk, B. Hammouti, H. Zarrok, S.S. Al-Deyab, M. Messali, *Int. J. Electrochem. Sci.* 6 (2011) 6261.
24. M. Lebrini, F. Bentiss, H. Vezin, M. Lagrenée, *Corros. Sci.* 48 (2006) 1279.
25. M. Lebrini, M. Lagrenée, H. Vezin, M. Traisnel, F. Bentiss, *Corros. Sci.* 49 (2007) 2254.
26. H. Zarrok, R. Saddik, H. Oudda, B. Hammouti, A. El Midaoui, A. Zarrouk, N. Benchat, M. Ebn Touhami, *Der Pharm. Chem.* 3 (2011) 272.
27. I. El Ouali, B. Hammouti, A. Aouniti, Y. Ramli, M. Azougagh, E. M. Essassi, M. Bouachrine, *J. Mater. Envir. Sci.* 1 (2010) 1.
28. A. Zarrouk, B. Hammouti, A. Dafali, H. Zarrok, R. Touzani, M. Bouachrine, M. Zertoubi, *Res. Chem. Intermed.* (2011) DOI 10.1007/s11164-011-0444-2
29. F.Z. Bouanis, F. Bentiss, M. Traisnel, C. Jama, *Electrochim. Acta.* 54 (2009) 2371.
30. M.S. Morad, A.M.K. El-Dean, *Corros. Sci.* 48 (2006) 3398.
31. K. Tebbji, B. Hammouti, H. Oudda, A. Ramdani, M. Benkadour, *Appl. Surf. Sci.* 252 (2005) 1378.
32. A. Yurt, A. Balaban, S. Ustun Kandemir, G. Bereket, B. Erk, *Mater. Chem. Phys.* 85 (2004) 420.
33. F. Bentiss, C. Jama, B. Mernari, H. El Attari, L. El Kadi, M. Lebrini, M. Traisnel, M. Lagrenée, *Corros. Sci.* 51 (2009) 1628.
34. A.K. Satpati, P.V. Ravindran, *Mater. Chem. Phys.* 109 (2008) 352.
35. A.R.S. Priya, V.S. Muralidharam, A. Subramania, *Corrosion.* 64 (2008) 541.
36. P. Bommersbach, C. Alemany-Dumont, J.P. Millet, B. Normand, *Electrochim. Acta.* 51 (2006) 4011.
37. M.S. Morad, *Corros. Sci.* 42 (2000) 1307.
38. K. Jutner, *Electrochim. Acta.* 10 (1990) 1501.
39. U. Rammelt, G. Reinhard, *Corros. Sci.* 27 (1987) 373.
40. J. Pang, A. Briceno, S. Chander, *J. Electrochem. Soc.* 137 (1990) 3447.
41. Z. Stoynov, *Electrochim. Acta.* 35 (1990) 1493.
42. J.R. Macdonald, *J. Electroanal. Chem.* 223 (1987) 25.
43. D.A. Lopez, S.N. Simison, S.R. de Sanchez, *Electrochim. Acta.* 48 (2003) 845.
44. J.W. Schultze, K. Wippermann, *Electrochim. Acta.* 32 (1987) 823.
45. F. Bentiss, M. Lebrini, M. Lagrenée, M. Traisnel, A. Elfarouk, H. Vezin, *Electrochim. Acta.* 52 (2007) 6865.
46. S. Martinez, M. Metikoš-Hukovic', *J. Appl. Electrochem.* 33 (2003) 137
47. M. Lebrini, F. Bentiss, N. Chihib, C. Jama, J.P. Hornez, M. Lagrenée, *Corros. Sci.* 50 (2008) 2914.
48. F. Bentiss, M. Lagrenée, M. Traisnel, J.C. Hornez, *Corros. Sci.* 41 (1999) 789.
49. E. McCafferty, N. Hackerman, *J. Electrochem. Soc.* 119 (1972) 146.
50. P. Li, J.Y. Lin, K.L. Tan, J.Y. Lee, *Electrochim. Acta.* 42 (1997) 605.
51. S.S. Abdel Rehim, O.A. Hazzazi, M.A. Amin, K.F. Khaled, *Corros. Sci.* 50 (2008) 2258.
52. I. Ahamad, R. Prasad, M.A. Quraishi, *Corros. Sci.* 52 (2010) 933.
53. F. Bentiss, M. Outirite, M. Traisnel, H. Vezin, M. Lagrenée, B. Hammouti, S.S. Al-Deyab, C. Jama, *Int. J. Electrochem Sci.* 7 (2012) 1699.
54. I.B. Obot, N.O. Obi-Egbedi, S.A. Umoren, *Corros. Sci.* 51 (2009) 1868.
55. L. Herrag, B. Hammouti, S. Elkadiri, A. Aouniti, C. Jama, H. Vezin, F. Bentiss, *Corros. Sci.* 52 (2010) 3042.
56. M. Behpour, S.M. Ghoreishi, N. Soltani, M. Salavati-Niasari, M. Hamadani, A. Gandomi, *Corros. Sci.* 50 (2008) 2172.

57. M. Sahin, S. Bilgic, H. Yilmaz, *Appl. Surf. Sci.* 195 (2002) 1
58. M. Kaminski, Z. Szklarska-Smialowska, *Corros. Sci.* 13 (1973) 557.
59. O. Olivares, N.V. Likhanova, B. Gomez, J. Navarrete, M.E. Llanos- Serrano, E. Arce, J.M. Hallen, *Appl. Surf. Sci.* 252 (2006) 2894.
60. O.K. Abiola, Oforika, *Mater. Chem. Phys.* 83 (2004) 315.
61. M. Ozcan, N.C. Solmaz, G. Kardas, I. Dehri, *Colloid. Surf. A.* 325 (2008) 57.
62. X. Li, S. Deng, H. Fu, T. Li, *Electrochim. Acta.* 54 (2009) 4089.
63. H. Ashassi-Sorkhabi, B. Shaabani, D. Seifzadeh, *Appl. Surf. Sci.* 239 (2005) 154.
64. D. Schweinsberg, G. George, A. Nanayakkara, D. Steinert, *Corros. Sci.* 28 (1988) 33.
65. A. Fouda, M. Moussa, F.I. Taha, A.I. ElNeanaa, *Corros. Sci.* 26 (1986) 719.
66. G. Banerjee, S.N. Malhotra, *Corrosion.* 48 (1992) 10.